Check for updates

https://doi.org/10.4047/jap.2026.18.2.131

Optimizing adhesive protocols for CAD-CAM restorations: Is simplification a reliable alternative to conventional silane application?

Soner Sismanoglu*
Department of Restorative Dentistry, Faculty of Dentistry, Istanbul University-Cerrahpasa, Istanbul, Turkey

ORCID
Soner Sismanoglu
https://orcid.org/0000-0002-1272-5581

PURPOSE. This *in vitro* study compared the bond strength and surface morphology of CAD-CAM restorative materials treated with different silane-based strategies, evaluating the influence of material type and artificial aging. **MATERIALS AND METHODS.** Five CAD-CAM materials were evaluated: leucite-reinforced glass ceramic (LEU), lithium disilicate (LDS), zirconia-reinforced lithium silicate (ZLS), polymer-infiltrated ceramic network (PICN), and resin nanoceramic (RNC). A total of 315 specimens (63 per material) were assigned to five groups: conventional silane application (G1, positive control), silane-containing universal adhesive (G2), single-step cementation with silane-containing self-adhesive resin cement (G3), self-etching ceramic primer (G4), and no silane application (G5, negative control). Two resin cylinders were bonded to each specimen and tested either immediately or after 10,000 thermal cycles. Micro-shear bond strength testing was performed, failure modes were analyzed microscopically, and representative specimens were examined by scanning electron microscopy. Statistical analysis was conducted using linear mixed-effects models with post-hoc Tukey tests and planned contrasts ($\alpha = .05$). **RESULTS.** Material type, bonding strategy, aging, and their interactions significantly affected bond strength ($P < .001$). The conventional protocol (G1) consistently yielded the highest values across all materials, while negative controls showed the lowest. Simplified strategies demonstrated intermediate values that were generally lower than G1 but remained within clinically acceptable ranges (15 – 25 MPa). Thermal cycling reduced bond strength in all groups, although the relative ranking of protocols was preserved. SEM analysis revealed material-dependent surface characteristics. **CONCLUSION.** The conventional three-step silane protocol remains the most reliable approach for durable bonding, while simplified strategies may represent acceptable alternatives depending on the material. [J Adv Prosthodont 2026;18:131-44]

KEYWORDS
Dental bonding; Ceramics; Computer-aided design; Shear strength; Silane coupling agents

Corresponding author
Soner Sismanoglu
Department of Restorative Dentistry, Faculty of Dentistry, Istanbul University-Cerrahpasa, Cerrahpasa Campus, Kocamustafapasa Cad., No:53, 34098, Fatih/Istanbul, Turkey
Tel +905423209950
E-mail soner.s@hotmail.com

Received December 24, 2025 /
Last Revision January 24, 2026 /
Accepted February 11, 2026

© 2026 The Korean Academy of Prosthodontics
This is an Open Access article distributed under the terms of the Creative Commons Attribution Non-Commercial License (https://creativecommons.org/licenses/by-nc/4.0) which permits unrestricted non-commercial use, distribution, and reproduction in any medium, provided the original work is properly cited.

https://doi.org/10.4047/jap.2026.18.2.131

INTRODUCTION

Computer-aided design-computer-aided manufacturing (CAD-CAM) ceramic restorations have revolutionized restorative dentistry by offering superior mechanical properties, esthetics, and clinical efficiency compared with traditional techniques.[1] The long-term success of these restorations depends on establishing durable resin-ceramic bonds through a combination of mechanical and chemical mechanisms.[2] The standard adhesive protocol for silica-based ceramics involves hydrofluoric acid etching to create micromechanical retention, followed by silane coupling to establish chemical bonds with resin-based luting agents.[3,4] The most widely used silane, γ-methacryloxypropyltrimethoxysilane (γ-MPTS), is a bifunctional molecule that forms siloxane bonds with hydroxylated ceramic surfaces while also copolymerizing with methacrylate groups in adhesive resins.[5,6] This dual mechanism has long been regarded as the gold standard, consistently achieving high bond strength and excellent clinical longevity.[7] Clinical success typically requires bond strengths exceeding 15 – 25 MPa to ensure long-term restoration survival.[8]

However, the multi-step nature of this protocol requires technical sensitivity, is time-consuming, and is prone to contamination between application steps.[9] To address these drawbacks, simplified adhesive strategies have been introduced, including silane-containing universal adhesives, silane-containing self-adhesive resin-based luting agent, and self-etching ceramic primers. Universal adhesives aim to eliminate the need for separate silane application by incorporating γ-MPTS or similar agents directly into the adhesive system, often in combination with 10-methacryloyloxydecyl dihydrogen phosphate (MDP), which enables bonding to tooth substrates, metal oxides, and zirconia.[9-11] While some studies report adequate immediate bond strengths,[12] others show reduced durability after artificial aging, raising concerns about long-term performance.[3,13] These shortcomings have been attributed in the literature to the acidic pH of universal adhesives, which may accelerate silane hydrolysis,[5,14] and to their relatively high viscosity, which may hinder infiltration into microretentive features.[14,15] Consequently, many clinicians continue to apply a separate silane step even when using universal adhesives.

A second simplification strategy involves silane-containing self-adhesive resin-based luting agent. PANAVIA SA Cement Universal (Kuraray Noritake) is a notable example, combining MDP for bonding to tooth structure and zirconia with a proprietary long-chain silane (LCSi) for glass ceramics.[16] This dual-monomer system allows single-step cementation without primers or separate silane application. Although preliminary results are promising,[17] large-scale comparative studies remain limited. A third approach eliminates hydrofluoric acid entirely through single-component self-etching ceramic primers. For instance, Monobond Etch & Prime (Ivoclar Vivadent) uses ammonium polyfluoride to simultaneously etch ceramic surfaces and deposit silane.[18-21] This strategy reduces the safety risks of hydrofluoric acid and decreases technique sensitivity and chairside time.[22,23] However, evidence remains conflicting: while some studies report bond strengths comparable to the conventional acid + silane protocol,[24] others show significantly weaker results.[21,25,26] Interestingly, some reports suggest that self-etching primers may offer improved long-term stability due to their less aggressive etching patterns.[27]

The wide range of CAD-CAM materials further complicates the selection of adhesive strategies. Leucite-reinforced glass ceramics, lithium disilicate ceramics, polymer-infiltrated ceramic networks (PICN), resin nanoceramics (RNC), and zirconia-reinforced lithium silicate ceramics exhibit distinct microstructural characteristics and adhesive challenges.[1,28-30] For example, RNCs such as Lava Ultimate respond poorly to silane due to their resin-rich matrix,[31] whereas zirconia-reinforced lithium silicate ceramics may benefit from primers containing both silane and MDP.[30,32-34] Despite the clinical importance of simplified adhesive strategies, systematic comparative studies are scarce. Most investigations evaluate only one or two approaches, often on a single material type and with short-term testing, limiting the ability to draw evidence-based conclusions.[7] Current evidence suggests that outcomes are highly

material-dependent: while some ceramics perform adequately with simplified methods, others still require conventional multi-step protocols to ensure durable long-term bonding.[12,28]

Aging behavior is another critical factor. Thermal cycling, which simulates intraoral temperature fluctuations, reduces bond strength through differential thermal expansion and hydrolytic degradation at the resin-ceramic interface.[33,35-37] Such conditions often reveal weaknesses not apparent in immediate testing, particularly in silane-mediated bonds.[3] Importantly, no previous study has systematically compared the four main silane strategies—separate silane application, silane-containing universal adhesives, silane-containing self-adhesive resin-based luting agent, and self-etching ceramic primers—under standardized conditions. Moreover, the material-specific effectiveness of each approach and the long-term stability of simplified protocols remain poorly understood.

From a clinical perspective, the selection of an appropriate bonding protocol should be tailored to the clinical scenario. Restorations with limited macromechanical retention or those subjected to high functional stresses require maximum bond durability and may benefit mostly from conventional multi-step protocols. Conversely, simplified approaches may represent acceptable alternatives for adequately retained full-coverage restorations or minimally stressed applications where procedural efficiency is prioritized. Understanding the performance of simplified protocols under standardized aging conditions is therefore essential for evidence-based protocol selection. Therefore, the aim of this study was to directly compare four silane strategies and a negative control across five representative CAD-CAM materials, evaluating both immediate and aged bond performance. The findings are expected to provide evidence-based guidance for clinicians in selecting optimal adhesive strategies and support the development of simplified yet reliable cementation protocols. The null hypotheses tested were: (1) the silane protocol would not significantly affect bond strength to CAD-CAM materials, (2) CAD-CAM material type would not influence the relative effectiveness of different adhesive protocols, and (3) thermal cycling would not significantly affect bond strength or alter the relative performance ranking of the bonding protocols.

MATERIALS AND METHODS

Study design and specimen preparation

In this *in vitro* experimental study, the micro-shear bond strength (μSBS) of five different silane protocols on five CAD-CAM materials was evaluated using a three-factor mixed factorial design: Material (5 levels), Method (5 levels), and Aging (2 levels: Immediate vs. Thermal cycling).

The specimen size was determined based on an a priori power analysis using data from a previous study.[38] Assuming α =.05, statistical power = .80, and a medium effect size (f = .25), a minimum of 12 specimens per group was calculated to be sufficient.

Five CAD-CAM materials with distinct microstructures were selected: zirconia-reinforced lithium silicate glass ceramic (Celtra Duo; Dentsply Sirona; ZLS), lithium disilicate glass ceramic (IPS e.max CAD; Ivoclar Vivadent; LDS), leucite-reinforced glass ceramic (IPS Empress CAD; Ivoclar Vivadent; LEU), resin nanoceramic (Lava Ultimate; 3M ESPE; RNC), and polymer-infiltrated ceramic network (VITA Enamic; VITA Zahnfabrik; PICN). Comprehensive details on CAD-CAM materials are provided in Table 1.

The blocks were sectioned into 2 mm-thick slices using a water-cooled precision cutting device (IsoMet High Speed Pro; Buehler). LDS and ZLS specimens were crystallized following manufacturer guidelines, while LEU, PICN, and RNC were tested in their as-received state. After sectioning (and crystallization where applicable), the specimens were embedded in cold-curing acrylic resin within molds fabricated by a 3D printer using PLA material, ensuring that the bonding surface remained exposed. The surfaces were polished with 600-grit silicon carbide paper under water cooling to obtain a standardized flat surface for bonding.

Sixty specimens were prepared for each material (12 per method group). Two resin cylinders (one for Immediate and one for Thermal cycling testing) were bonded to each specimen, yielding a total of 120 measurements per material. Additionally, three specimens from each material were allocated for scanning

https://doi.org/10.4047/jap.2026.18.2.131

Table 1. Materials used in the study

Material	Manufacturer; LOT	Type	Composition
Celtra DUO; ZLS	DeguDent GmbH, Hanau-Wolfgang, Germany; 18031525	Zirconia-reinforced lithium silicate glass ceramic	SiO_2 (58%), Li_2O (18.5%), ZrO_2 (10.1%), P_2O_5 (5%), CeO_2 (2%), Al_2O_3 (1.9%), Tb_4O_7 (1%).
IPS e.max CAD; LDS	Ivoclar Vivadent AG, Schaan, Liechtenstein; Z00921	Lithium disilicate glass ceramic	SiO_2 (57 – 80%), Li_2O (11 – 19%), K_2O (0 – 13 %wt), P_2O_5 (0 – 11%), ZrO_2 (0 – 8%), ZnO (0 – 8%), Al_2O_3 (0 – 5%) MgO (0 – 5%), coloring oxides (0 – 8% by weight).
IPS Empress CAD; LEU	Ivoclar Vivadent AG, Schaan, Liechtenstein; Y45442	leucite-reinforced glass ceramic	SiO_2 (60 – 65 %wt), Al_2O_3 (16 – 20 %wt), K_2O (10 – 14 %wt), Na_2O (3.5 – 6.5 %wt), other oxides (0.5 – 7 % wt), pigments (0.2 – 1 %wt).
Lava Ultimate; RNC	3M ESPE, St. Paul, MN, USA; N619802	Resin nanoceramic	Bis-GMA, UDMA, Bis-EMA, TEGDMA. Filler: ZrO_2 (4 – 11 nm) and SiO_2 (20 nm), aggregated zirconia/silica cluster filler, 80% by weight.
Vita Enamic; PICN	VITA Zahnfabrik H. Rauter, Bad Sackingen, Germany; 51540	Polymer-infiltrated ceramic network	UDMA, TEGDMA. Filler: Feldspar ceramic enriched with aluminum oxide, 86% by weight.

Bisphenol A polyethylene glycol diether dimethacrylate (Bis-EMA), Bisphenol A diglycidylmethacrylate (Bis-GMA), Triethylene glycol dimethacrylate (TEGDMA), Urethane dimethacrylate (UDMA).

electron microscopy (SEM): one untreated control, one with respective surface treatment (hydrofluoric acid etching for glass-ceramics or airborne-particle abrasion for resin nanoceramic), and one treated with self-etching ceramic primer (Monobond Etch & Prime). Thus, 63 specimens per material were obtained, totaling 315 (300 for bond testing and 15 for SEM).

Surface treatments and experimental groups

Surface treatments were performed according to manufacturer recommendations. Etching times, primer application durations, and material-specific protocols were strictly followed as specified by the respective manufacturers to ensure clinical relevance and reproducibility. All glass-ceramic materials were etched with 9% buffered hydrofluoric acid (Porcelain Etchant; Ultradent): 20 s for LEU, 20 s for LDS, 60 s for PICN, and 30 s for ZLS, followed by rinsing with water for 60 s and air drying. RNC specimens were treated with airborne-particle abrasion using 50 μmAl_2O_3 (Cobra; Renfert) at 2 bar pressure, 10 mm distance, and 10 s duration, and then subsequently ultrasonically cleaned in distilled water and dried with air (excluding Group 5). Specimens were randomly assigned to five groups (n = 12):

Group 1 (G1; conventional three-step, positive control): After surface treatment, a silane coupling agent (Porcelain Primer; Bisco) was applied for 20 s and air-dried for 5 s. An adhesive (Porcelain Bonding Resin; Bisco) was then applied and light-cured for 10 s. Finally, cylinders were built using a dual-cure resin-based luting agent (RelyX Ultimate; 3M ESPE).

Group 2 (G2; silane-containing universal adhesive): After surface treatment, a silane-containing universal adhesive (Single Bond Universal; 3M ESPE) was applied for 20 s and air-dried for 5 s. Cylinders were then built using RelyX Ultimate.

Group 3 (G3; silane-containing self-adhesive resin-based luting agent, single-step): After surface treatment, a silane-containing self-adhesive resin-based luting agent (PANAVIA SA Cement Universal) was directly applied to build the cylinders. It should be noted that this group represents a complete cementation strategy employing a chemically distinct luting agent, rather than isolated silane incorporation, as the cement contains both silane (LCSi) and MDP functional monomers.

Group 4 (G4; self-etching ceramic primer): Etching with hydrofluoric acid was omitted for glass-ceramics (LEU, LDS, PICN, ZLS). Instead, a self-etching ceramic primer (Monobond Etch & Prime) was applied with a microbrush for 20 s, allowed to react for 40 s, rinsed with water for 30 s, and air-dried. For RNC, Monobond Etch & Prime was applied directly without prior airborne-particle abrasion, maintaining consistency with the chemical-only surface treatment approach of this group. Cylinders were then built using RelyX Ultimate.

Group 5 (G5; negative control, no silane): After surface treatment, a silane-free adhesive (Porcelain Bonding Resin; Bisco) was applied and light-cured for 10 s. Cylinders were then built using RelyX Ultimate.

Bond strength evaluation (micro-shear test)

Two resin cylinders (0.8 mm diameter × 1.0 mm height) were constructed on each specimen surface using transparent polyethylene tube molds. Cylinders were fabricated with the assigned resin-based luting agent and light-cured for 20 s with an LED curing unit (Elipar; 3M ESPE; 1,200 mW/cm^2). Specimens were stored in distilled water at 37°C for 24 h. Subsequently, one cylinder per specimen was tested immediately, while the other underwent thermal cycling (10,000 cycles, 5 – 55°C, 30 s dwell time, 10 s transfer time).

μSBS testing was performed using a dedicated micro-shear bond strength testing device (Esetron) with a crosshead speed of 0.5 mm/min. Bond strength was calculated as: μSBS (MPa) = F (N) / A (mm^2), where F = fracture load and A = bonded area.

Fractured surfaces were examined at 40× magnification with a stereomicroscope (SMZ745T; Nikon). Failure modes were classified as adhesive (failure at the resin-ceramic interface), cohesive in ceramic (failure within the ceramic substrate), cohesive in cement (failure within the resin cement), or mixed.

Surface characterization (SEM)

Three specimens from each material (15 in total) were prepared for SEM analysis: one untreated control, one subjected to the respective manufacturer-recommended surface treatment (hydrofluoric acid etching for glass-ceramics; airborne-particle abrasion for resin nanoceramic), and one treated with the self-etching ceramic primer (Monobond Etch & Prime). This allocation allowed direct comparison of surface topographies corresponding to the bonding protocols evaluated in the bond strength experiments. Specimens were sputter-coated with a thin gold layer (Polaron SC7620; ThermoVG Scientific). They were then examined under SEM (JEOL 5500; JEOL Inc) at 10 kV accelerating voltage. Surface topography was assessed at 1,000× and 5,000× magnifications.

Statistical analysis

Statistical analyses were performed using linear mixed-effects (LME) modeling to account for the hierarchical structure of repeated measurements (two cylinders per specimen; within-specimen Aging). The dependent variable was bond strength (MPa); Material (5 levels: LEU, LDS, PICN, RNC, ZLS), Method (5 levels), and Aging (Immediate vs. Thermal cycling) were fixed effects, including all two- and three-way interactions. Specimen was modeled as a random intercept nested within Material × Method.

Estimated marginal means were obtained from the fitted LME model, and Tukey-adjusted post-hoc comparisons were conducted. Additionally, the Method factor was re-coded as Separate, Incorporated, and None, and planned contrasts were performed for (i) Separate vs. Incorporated, (ii) Incorporated vs. None, and (iii) Separate vs. None. Results were reported as mean differences (Δ), 95% confidence intervals, and Holm-adjusted P-values. Failure mode distributions were compared between Immediate and Thermal cycling using chi-square tests on pooled data across all materials and bonding protocols. All analyses were conducted in R (v.4.5.1; R Foundation for Statistical Computing, Vienna, Austria) using the lme4 and emmeans packages.

RESULTS

Bond strength analysis

Linear mixed-effects analysis showed that the three main effects—Material, Method, and Aging—were statistically significant predictors of μSBS (all P < .001; Table 2). All two-way interactions (Material × Method, Material × Aging, Method × Aging) and the three-way interaction (Material × Method × Aging)

https://doi.org/10.4047/jap.2026.18.2.131

Table 2. Linear mixed-effects model omnibus tests (Likelihood-ratio χ^2)

Effect	df	LR χ^2	*P*-value	Sig.
Material	40	1757.8	*P* < .001	***
Group (Method)	40	1750.9	*P* < .001	***
Aging	25	1244.6	*P* < .001	***
Material × Group	32	951.2	*P* < .001	***
Material × Aging	20	126.0	*P* < .001	***
Group × Aging	20	264.1	*P* < .001	***
Material × Group × Aging	16	48.6	*P* < .001	***

Note: Likelihood-ratio χ^2 tests were conducted using a linear mixed-effects model with Material, Method (Group), and Aging as fixed effects, and Specimen as a random intercept. This random effect accounts for the paired immediate and thermal cycling measurements obtained from the same specimen. For each effect, the full model was compared against a reduced model with the respective term removed, using maximum likelihood (ML) estimation. df denotes the difference in fixed-effect parameters between models. Significance levels: ***P < .001; **P < .01; *P < .05; ns = not significant.

were also significant (all P < .001). The results show that adhesive protocols behaved differently across ceramics, and the effect of thermal cycling was influenced by both the material and the protocol.

Estimated marginal means and post-hoc comparisons are summarized in Table 3. Within each ceramic group, the conventional three-step silane protocol (G1) consistently produced the highest immediate bond strength values, whereas the negative control groups (G5, silane-free) yielded the lowest. Notably, all bonding protocols except the negative control achieved bond strengths exceeding the commonly cited clinical threshold of 15 MPa, with G1 values ranging from 23.98 to 34.58 MPa across materials. The performance differences between G1 and simplified strategies (G2, G3) ranged from 2.0 to 6.5 MPa depending on the material, which may be clinically relevant for high-stress or retention-limited restorations. The silane-containing universal adhesive (G2) and the silane-containing self-adhesive resin-based luting agent (G3) produced intermediate outcomes, with no significant differences between them in several materials. After thermal cycling, a significant decrease in bond strength was observed across all groups (Δ = -3.4 to -5.5 MPa, all P < .001, Holm-adjusted). Despite this decrease, the relative ranking of adhesive protocols remained unchanged: G1 retained superiority, while G5 consistently exhibited the weakest performance. Among the tested ceramics, IPS e.max CAD demonstrated the highest absolute bond strengths both before and after artificial aging, whereas Lava Ultimate and Celtra Duo generally showed lower values.

Failure mode distributions across all materials did not differ significantly between Immediate and Thermal cycling conditions (chi-square test, P > .05; Table 4). Although no statistically significant differences were detected, a general trend toward more adhesive failures and fewer cohesive/mixed failures was observed after artificial aging. Groups associated with higher bond strengths (e.g., G1 in IPS Empress CAD, Lava Ultimate, and Celtra Duo) exhibited relatively more cohesive failures, whereas G5, which yielded the lowest strengths, was predominantly characterized by adhesive failures. The MEP group (G4) displayed a failure mode distribution similar to mid-to-high strength groups, though adhesive failures became more prevalent after thermal cycling. Cohesive failures occurred predominantly within the resin cement rather than the ceramic substrate. No cohesive failures within the ceramic material were observed across all groups and materials. These observations are consistent with bond strength outcomes, confirming the relationship between higher bond values and an increased likelihood of cohesive failure.

Planned comparisons (Separate = G1, Incorporated = G2 + G3, MEP = G4, None = G5) are presented in Table 5. Under both Immediate and Thermal cycling conditions, G1 produced significantly higher bond strength than Incorporated (Δ = 2.0 – 2.5 MPa, P < .001), while Incorporated was superior to G5 (Δ = 7.3 – 7.7 MPa,

Table 3. Microshear bond strength (MPa) of resin-ceramic interfaces for each material and bonding method under immediate and thermal cycling conditions, with within-material Tukey groupings

Material	Group	Imm mean ± SD (CI)	TC mean ± SD (95% CI)	Δ (TC-Imm) (MPa)
ZLS	G1	23.98 ± 2.94 (22.10-25.85) [a]	20.18 ± 2.78 (18.41-21.95) [a]	-3.79 ***
	G2	22.18 ± 3.03 (20.26-24.11) [b]	17.97 ± 2.60 (16.32-19.62) [b]	-4.22 ***
	G3	25.27 ± 2.97 (23.39-27.16) [c]	21.33 ± 2.78 (19.57-23.10) [c]	-3.94 ***
	G4	20.46 ± 1.82 (19.30-21.62) [e]	18.54 ± 1.77 (17.42-19.66) [b]	-1.92 ***
	G5	17.59 ± 3.02 (15.67-19.51) [d]	12.62 ± 2.68 (10.92-14.33) [d]	-4.97 ***
LDS	G1	29.61 ± 3.91 (27.12-32.10) [a]	26.30 ± 3.89 (23.83-28.77) [a]	-3.31 ***
	G2	24.96 ± 3.80 (22.55-27.37) [b]	20.37 ± 2.86 (18.55-22.18) [b]	-4.59 ***
	G3	24.23 ± 3.71 (21.88-26.59) [bc]	19.87 ± 3.27 (17.79-21.95) [b]	-4.37 ***
	G4	23.85 ± 2.22 (22.44-25.26) [c]	23.88 ± 2.20 (22.49-25.28) [d]	.03 ns
	G5	19.19 ± 3.99 (16.65-21.73) [d]	13.70 ± 3.38 (11.55-15.85) [c]	-5.49 ***
LEU	G1	34.58 ± 3.67 (32.25-36.91) [a]	31.15 ± 3.50 (28.93-33.37) [a]	-3.43 ***
	G2	29.80 ± 2.80 (28.02-31.58) [b]	24.58 ± 2.75 (22.84-26.33) [b]	-5.22 ***
	G3	27.82 ± 2.88 (25.99-29.66) [c]	23.34 ± 2.72 (21.61-25.07) [c]	-4.48 ***
	G4	28.46 ± 2.71 (26.74-30.18) [c]	26.66 ± 2.57 (25.03-28.29) [e]	-1.80 ***
	G5	21.33 ± 4.23 (18.64-24.02) [d]	15.76 ± 2.83 (13.96-17.56) [d]	-5.58 ***
RNC	G1	28.95 ± 3.24 (26.89-31.01) [a]	23.66 ± 2.73 (21.92-25.39) [a]	-5.29 ***
	G2	29.83 ± 3.17 (27.82-31.85) [a]	24.17 ± 3.08 (22.21-26.12) [a]	-5.67 ***
	G3	29.79 ± 3.13 (27.80-31.77) [a]	23.81 ± 3.10 (21.85-25.78) [a]	-5.98 ***
	G4	27.03 ± 3.02 (25.16-28.89) [c]	24.48 ± 2.85 (22.77-26.18) [b]	-2.55 ***
	G5	21.46 ± 3.73 (19.36-23.55) [b]	15.48 ± 3.58 (13.47-17.49) [b]	-5.98 ***
PICN	G1	27.86 ± 3.72 (25.51-30.21) [a]	24.36 ± 3.45 (22.19-26.54) [a]	-3.50 ***
	G2	23.67 ± 3.66 (21.39-25.95) [b]	19.56 ± 3.42 (17.45-21.67) [b]	-4.11 ***
	G3	22.95 ± 3.71 (20.66-25.24) [b]	18.47 ± 3.39 (16.39-20.55) [b]	-4.48 ***
	G4	20.90 ± 2.37 (19.45-22.34) [d]	20.01 ± 2.27 (18.64-21.39) [d]	-.89 ns
	G5	17.86 ± 4.86 (14.83-20.88) [c]	12.38 ± 4.10 (10.00-14.77) [c]	-5.48 ***

Note: Values are presented as mean ± standard deviation (SD) with 95% confidence intervals (CI).
Letters indicate the results of Tukey's HSD post-hoc test within each material; groups sharing a superscript letter are not significantly different at α = .05.
Δ denotes the mean difference between immediate and thermal cycling values for the same specimens. p-values were obtained from paired t-tests and adjusted for multiple comparisons using the Holm-Bonferroni method. ***P < .001; **P < .01; *P < .05; ns = not significant.
Abbreviations: Imm, immediate, TC, thermal cycling.

P < .001). Consequently, G1 consistently outperformed G5 (Δ = 9.3 – 10.1 MPa, P < .001). Interaction terms indicated small but statistically significant reductions in these differences after artificial aging (–0.38 to –0.85 MPa, all P < .05). However, the overall ranking (G1 > Incorporated > G4 > G5) was preserved. Estimated marginal means are shown in Figure 1. The Separate method achieved the highest bond strength values, followed by MEP and Incorporated, while the None group (G5) consistently yielded the lowest. All pairwise analyses yielded significant differences (P < .001; Table 5). Thermal cycling reduced bond strength across all methods, but the relative ranking among protocols was maintained. It should be emphasized that the values in Figure 1 represent model-based marginal estimates from the LME analysis, with equal weighting of materials to ensure balanced comparisons, rather than raw means.

Surface topography (SEM analysis)

SEM micrographs (Figure 2) at 1,000× magnification revealed smooth, homogeneous surfaces in untreated controls across all materials. At 5,000× magnification, HF-etched glass-ceramics (LEU, LDS, PICN)

https://doi.org/10.4047/jap.2026.18.2.131

Table 4. Failure mode distribution (Immediate vs. Thermal cycling)

Material	Group	Adhesive (Imm% / TC%)	Cohesive (Imm% / TC%)	Mixed (Imm% / TC%)
ZLS	G1	33.3 / 58.3	41.7 / 25.0	25.0 / 16.7
	G2	41.7 / 66.7	33.3 / 25.0	25.0 / 8.3
	G3	25.0 / 50.0	50.0 / 33.3	25.0 / 25.0
	G4	41.7 / 66.7	33.3 / 25.0	25.0 / 8.3
	G5	83.3 / 91.7	8.3 / 0.0	8.3 / 8.3
LDS	G1	33.3 / 50.0	41.7 / 33.3	25.0 / 16.7
	G2	41.7 / 58.3	33.3 / 25.0	25.0 / 16.7
	G3	25.0 / 41.7	50.0 / 33.3	25.0 / 25.0
	G4	41.7 / 58.3	33.3 / 25.0	25.0 / 16.7
	G5	66.7 / 75.0	16.7 / 16.7	16.7 / 8.3
LEU	G1	25.0 / 41.7	50.0 / 33.3	25.0 / 25.0
	G2	33.3 / 58.3	41.7 / 25.0	25.0 / 16.7
	G3	25.0 / 50.0	50.0 / 33.3	25.0 / 16.7
	G4	33.3 / 58.3	41.7 / 25.0	25.0 / 16.7
	G5	75.0 / 83.3	16.7 / 8.3	8.3 / 8.3
RNC	G1	25.0 / 50.0	50.0 / 33.3	25.0 / 16.7
	G2	33.3 / 41.7	41.7 / 33.3	25.0 / 25.0
	G3	25.0 / 50.0	50.0 / 33.3	25.0 / 16.7
	G4	33.3 / 41.7	41.7 / 33.3	25.0 / 25.0
	G5	83.3 / 91.7	8.3 / 0.0	8.3 / 8.3
PICN	G1	33.3 / 58.3	41.7 / 25.0	25.0 / 16.7
	G2	25.0 / 50.0	50.0 / 33.3	25.0 / 16.7
	G3	25.0 / 41.7	50.0 / 33.3	25.0 / 25.0
	G4	33.3 / 58.3	41.7 / 25.0	25.0 / 16.7
	G5	66.7 / 75.0	16.7 / 16.7	16.7 / 8.3

Note: Values are expressed as percentages of specimens (Immediate [Imm%] / Thermal cycling [TC%]); each group included 12 specimens. Failure types were defined as follows: Adhesive = failure at the ceramic-resin interface; Cohesive = failure within the ceramic or resin; Mixed = combination of adhesive and cohesive failure.

Table 5. Planned contrasts of estimated marginal means (LME; averaged over materials)

Contrast	Imm Δ (MPa) (CI)	Imm *P*	TC Δ (MPa) (CI)	TC *P*
Incorporated - None	6.77 (6.32 to 7.21)	*P* < .001	7.31 (6.86 to 7.75)	*P* < .001
Separate - Incorporated	2.02 (1.58 to 2.47)	*P* < .001	2.62 (2.17 to 3.07)	*P* < .001
Separate - None	8.79 (8.27 to 9.31)	*P* < .001	9.93 (9.41 to 10.44)	*P* < .001
MEP - None	3.43 (2.92 to 3.95)	*P* < .001	6.75 (6.24 to 7.27)	*P* < .001
MEP - Incorporated	-3.34 (-3.78 to -2.89)	*P* < .001	-0.55 (-1.00 to -0.11)	*P* = .001
MEP - Separate	-5.36 (-5.87 to -4.84)	*P* < .001	-3.18 (-3.69 to -2.66)	*P* < .001
Interaction (contrast × aging)				
Incorporated - None × Aging	.54 (-.27 to 1.35)	*P* = .073 ns		
Separate - Incorporated × Aging	.60 (-.21 to 1.41)	*P* = .050 *		
Separate - None × Aging	1.14 (0.20 to 2.07)	*P* = .0003 ***		
MEP - None × Aging	3.32 (2.39 to 4.25)	*P* < .001 ***		
MEP - Incorporated × Aging	2.78 (1.97 to 3.59)	*P* < .001 ***		
MEP - Separate × Aging	2.18 (1.25 to 3.12)	*P* < .001 ***		

Note: Δ values are estimated mean differences (MPa) with 95% confidence intervals (CI) obtained from the linear mixed-effects (LME) model; positive values indicate superiority of the first-listed method. Immediate (Imm) and thermal cycling (TC) contrasts were adjusted for multiple testing using the Holm method. Interaction rows denote the change in contrast after aging (Immediate - Thermal cycling). Significance codes: ***$P < .001$; **$P < .01$; *$P < .05$; ns = not significant.

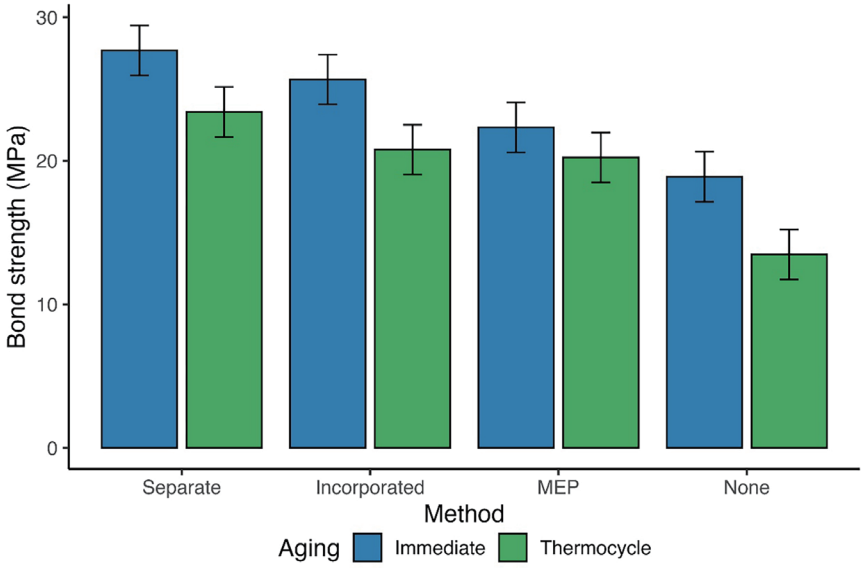


Fig. 1. Estimated marginal means of bond strength (MPa) for the four surface treatment methods (Incorporated, Separate, MEP and None). Values represent model-based estimates from linear mixed-effects analysis, averaged across all five ceramic materials with equal weighting to ensure balanced comparisons. Results are shown separately for Immediate and Thermal cycling artificial aging conditions. Error bars represent 95% confidence intervals. The plot illustrates the overall effect of bonding method independent of the material type, highlighting the superior performance of the Separate method and the consistently lower values of the Incorporated method across both aging conditions.

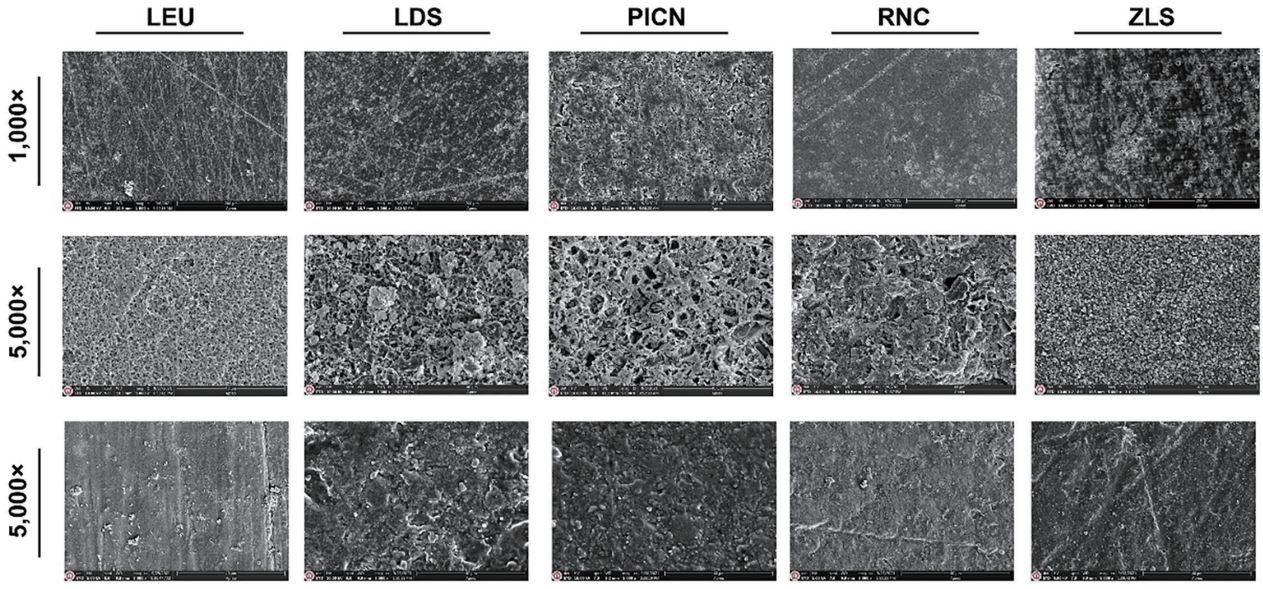


Fig. 2. Representative SEM images of CAD-CAM materials. Upper row: untreated control surfaces at ×1,000; middle row: conditioned surfaces at ×5,000 (hydrofluoric acid etching or airborne-particle abrasion); lower row: surfaces treated with Monobond Etch & Prime (MEP) at ×5,000. Hydrofluoric acid etching in LEU, LDS, and PICN generated honeycomb-like microporosities, whereas ZLS revealed a granular, spheroidal particle-like morphology. Airborne-particle abrasion of RNC created grooves and shallow craters accompanied by a laminar, flake-like appearance. In contrast, MEP produced a smoother surface morphology with reduced porosities, as most of the micro-irregularities were simultaneously infiltrated and filled with resin monomers, resulting in a more homogeneous appearance.

https://doi.org/10.4047/jap.2026.18.2.131

exhibited the expected honeycomb-like microporous topography, consistent with selective dissolution of the glass matrix. In contrast, ZLS specimens displayed a distinct granular, spheroidal particle-like topography instead of the classic honeycomb pattern, reflecting their zirconia-containing microstructure. For RNC specimens, airborne-particle abrasion did not create deep pores; instead, it produced irregular surfaces characterized by shallow craters, grooves, and a laminar, flake-like appearance, resembling layered surface peeling. This lamellar pattern differs from that of glass-ceramics and is likely attributable to the resin-rich matrix of the material.

At 5,000× magnification following application of the self-etching ceramic primer (MEP), a less pronounced etching pattern was observed compared to HF treatment. Although shallow microporosities were formed initially, these features were partially filled by the simultaneously delivered silane/adhesive components, resulting in smoother, more homogeneous surfaces. This effect was particularly evident in glass-ceramics, where the typical honeycomb-like topography was attenuated, and in RNC, where only minimal surface alterations were observed.

DISCUSSION

The development of simplified adhesive protocols for CAD-CAM restorations represents a significant advancement in restorative dentistry,[1,13] as these approaches address the limitations of traditional multi-step cementation. In this comprehensive study, five different silane protocols were systematically evaluated on representative CAD-CAM materials, providing an evidence-based framework for selecting optimal adhesive strategies. To our knowledge, this is the first study to directly compare the conventional three-step silane protocol, silane-containing universal adhesives, silane-containing self-adhesive resin-based luting agent, self-etching ceramic primers, and negative controls within a unified experimental design. The findings revealed notable variations in bond strength across the evaluated protocols.[28] All three null hypotheses were rejected: (1) the silane protocol had a significant effect on bond strength to CAD-CAM materials ($P < .001$), (2) the CAD-CAM material type significantly influenced the relative effectiveness of the adhesive protocols ($P < .001$ for Material × Method interaction), and (3) thermal cycling significantly reduced bond strength across all groups ($P < .001$), although the relative performance ranking of bonding protocols was preserved. The conventional three-step protocol consistently yielded the highest values, universal adhesives and self-adhesive resin-based luting agents showed intermediate performance, and negative controls produced the lowest results. The self-etching ceramic coupling agent (Monobond Etch & Prime) showed material-specific performance, yielding higher effectiveness with glass-ceramics but lower with resin nanoceramics.[19] After thermal cycling, all groups exhibited a reduction of 3.4 – 5.5 MPa, yet the overall ranking of adhesive strategies was preserved.[14,35]

The superior performance of the conventional three-step protocol aligns with previous literature highlighting the effectiveness of hydrofluoric acid etching followed by silane application.[4,10,28] This approach enhances micromechanical retention through controlled etching and strengthens chemical adhesion via dedicated silane deposition.[6] A separate silane step also allows for adequate solvent evaporation and silanol condensation, promoting the formation of a stable siloxane network at the interface.[6,20] The bond strength values obtained in this study were consistently high across all materials (LEU: 29.61 MPa, LDS: 34.58 MPa, PICN: 27.86 MPa, RNC: 28.95 MPa, ZLS: 23.98 MPa).[1] These values surpass the clinically acceptable threshold of 15 – 25 MPa,[8,39] offering substantial safety margins for long-term success.

Silane-containing universal adhesives showed intermediate performance, averaging 2.0 – 2.6 MPa lower than the conventional protocol.[3] This observation is consistent with systematic reviews reporting lower effectiveness compared to separate silane application.[5,13,14] The reduced performance has been attributed in the literature to the acidic pH (2.0 – 3.0), which accelerates silane hydrolysis and condensation, reducing the availability of reactive silanols.[5,11] Additionally, their relatively high viscosity may hinder penetration into etched microretentive features, thereby compromising micromechanical retention.[14,27] Nevertheless, universal adhesives

still achieved clinically acceptable values (> 20 MPa immediate, > 17 MPa aged),[3] supporting their use in routine restorations where procedural efficiency may be prioritized over marginal strength differences.[13]

Similarly, the silane-containing self-adhesive resin-based luting agent (PANAVIA SA Cement Universal) exhibited comparable performance to universal adhesives. It should be acknowledged that this group represents not only a different silane delivery strategy but also a chemically distinct luting agent with a dual monomer structure—incorporating MDP for adhesion to tooth structures and zirconia, and LCSi for glass-ceramics. Therefore, the observed performance reflects the combined effect of both the silane component and the overall cement chemistry, rather than isolated silane efficacy. Manufacturer data and independent studies report bond strengths approaching 35 – 40 MPa under optimal conditions.[29] In this study, strong results were observed particularly for lithium disilicate (27.82 MPa immediate) and leucite ceramics (24.23 MPa immediate).[16] Post-thermal-cycling stability was comparable to other simplified protocols, although reductions of 4.4 – 6.0 MPa underscore the importance of case selection.

Self-etching ceramic primers also showed material-dependent performance.[19] Immediate bond strengths of 17.59 – 21.33 MPa were obtained with glass-ceramics (LEU, LDS, PICN, ZLS). Although lower than those achieved with the conventional protocol, these values remained within clinically acceptable limits for *in vitro* assessment.[26] These findings align with previous reports suggesting comparable immediate values and potentially improved long-term stability.[19,27] The single-component approach also simplifies application and avoids the hazards of hydrofluoric acid.[18] However, performance with resin nanoceramic was significantly weaker (21.46 MPa immediate, 15.48 MPa aged),[23] consistent with prior studies on composite CAD-CAM blocks.[21] SEM analyses revealed smoother surfaces and reduced microporosity, which may explain the lower immediate values but could contribute to enhanced long-term stability.[19] Overall, these results emphasize that while the conventional three-step protocol remains the most consistent, simplified strategies may still offer clinically acceptable alternatives depending on the material and clinical context.

The significant Material × Method interaction further underscores the need for material-specific adhesive protocols.[28] Lithium disilicate consistently achieved the highest bond strengths, attributable to its favorable microstructure.[1,33] Resin nanoceramic, particularly with MEP, exhibited poor responsiveness due to its organic-rich, low-silica composition.[30,34] Zirconia-reinforced lithium silicate ceramics produced intermediate values, while PICN demonstrated stable performance across different protocols.[36] These findings confirm that adhesive strategies cannot be universally applied but must be tailored to each material.

From a clinical perspective, the conventional three-step protocol remains the gold standard, particularly for thin veneers, cantilever bridges, and restorations in high-stress regions.[1,38] Simplified strategies—universal adhesives, self-adhesive resin-based luting agents, and MEP—offer practical alternatives where procedural efficiency, safety, or patient considerations are prioritized.[13,18] The self-etching ceramic primer is especially valuable for glass-ceramics in cases where hydrofluoric acid is contraindicated, though case selection remains critical. Moreover, thermal cycling (10,000 cycles, 5 – 55°C) effectively simulated *in vitro* artificial aging and revealed an overall reduction in bond strength.[35] The universal decrease of 3.4 – 5.5 MPa highlights the importance of maximizing initial bond strength.[3,37] Importantly, the preservation of ranking order after artificial aging suggests that immediate performance may predict long-term outcomes,[14] although further clinical validation and additional aging protocols would be necessary to confirm durability in clinical settings. The greater vulnerability of simplified strategies to thermal stress indicates the need for conservative restoration designs or closer clinical monitoring.[13]

This study has several limitations. Although the *in vitro* design provided a controlled environment, it cannot fully replicate intraoral conditions such as occlusal loading, pH fluctuations, and biofilm activity.[13] Thermal cycling represents only one mode of artificial aging, and μSBS testing may not fully capture complex stress distributions.[28] While including MEP for resin nanoceramic ensured meth-

https://doi.org/10.4047/jap.2026.18.2.131

odological completeness, its clinical applicability is limited.[23] Future studies should incorporate additional artificial aging protocols such as mechanical loading, pH cycling, and microbial challenges, and explore novel silane formulations optimized for specific CAD-CAM materials.

CONCLUSION

Based on the findings of this *in vitro* study, it can be concluded that the conventional three-step silane protocol remains the most reliable approach for achieving durable resin-ceramic bonding across different CAD-CAM materials under the tested *in vitro* aging conditions. Although simplified bonding protocols, including universal adhesives, self-adhesive resin cements, and self-etching primers, demonstrated clinically acceptable bond strength values, these were generally lower and showed greater variability depending on the type of ceramic material used. Thermal cycling led to a reduction in bond strength in all experimental groups; however, the relative ranking of the bonding protocols remained unchanged, suggesting that immediate bond strength results may be predictive of long-term performance within the scope of *in vitro* thermocycling. From a clinical perspective, a careful balance between efficiency and reliability is required, as the conventional protocol demonstrated superior performance under artificial aging, whereas simplified approaches may serve as practical alternatives in selected clinical situations, especially when bonding glass-ceramic materials.

REFERENCES

1. Alhomuod M, Phark JH, Duarte S Jr. Bond strength to different CAD/CAM lithium disilicate reinforced ceramics. J Esthet Restor Dent 2023;35:129-37.
2. Yao C, Ahmed MH, De Grave L, Yoshihara K, Mercelis B, Okazaki Y, Van Landuyt KL, Huang C, Van Meerbeek B. Optimizing glass-ceramic bonding incorporating new silane technology in an experimental universal adhesive formulation. Dent Mater 2021;37:894-904.
3. Cardoso GC, Nakanishi L, Isolan CP, Rodrigues CS, Moraes RR. Bonding stability of universal adhesives to feldspathic ceramic with or without prior silane application. J Prosthodont 2024;33:918-25.
4. Nogueira IO, Oliveira PFG, Magno MB, Ferreira DMTP, Maia LC, Rabello TB. Does the application of an adhesive layer improve the bond strength of etched and silanized glass-ceramics to resin-based materials? A systematic review and meta-analysis. J Prosthet Dent 2021;125:56-64.
5. Yao C, Yu J, Wang Y, Tang C, Huang C. Acidic pH weakens the bonding effectiveness of silane contained in universal adhesives. Dent Mater 2018;34:809-18.
6. Zhang ZQ, Ren KF, Ji J. Silane coupling agent in biomedical materials. Biointerphases 2023;18:030801.
7. Turunç-Oğuzman R, Şişmanoğlu S. Influence of surface treatments and adhesive protocols on repair bond strength of glass-matrix and resin-matrix CAD/CAM ceramics. J Esthet Restor Dent 2023;35:1322-31.
8. Kazem NE, El-Refai DA, Alian G. Assessment of physical properties of bioactive glass-modified universal multimode adhesive and its bonding potential to artificially induced caries affected dentin. BMC Oral Health 2024;24:423.
9. Almaskin D, Alzaher ZA, Qaw M, Al-Thobity AM, Alshahrani A, Alsalman A, Akhtar S, Shetty AC, Gad MM. The bond strength of a universal adhesive system with silane to lithium disilicates in comparison with an isolated silane coupling agent. J Prosthodont 2022;31:512-20.
10. Cardenas AM, Siqueira F, Hass V, Malaquias P, Gutierrez MF, Reis A, Perdigão J, Loguercio A. Effect of MDP-containing silane and adhesive used alone or in combination on the long-term bond strength and chemical interaction with lithium disilicate ceramics. J Adhes Dent 2017;19:203-12.
11. Kim YR, Kim JH, Son SA, Park JK. Effect of silane-containing universal adhesives on the bonding strength of lithium disilicate. Materials (Basel) 2021;14:3976.
12. Doğan İ, Karaman E. How the repair bonding strength of hybrid ceramic CAD/CAM blocks is influenced by the use of surface treatments and universal adhesives. Dent Mater J 2024;43:312-9.
13. Lima RBW, Muniz IAF, Campos DES, Murillo-Gómez F, Andrade AKM, Duarte RM, de Souza GM. Effect of universal adhesives and self-etch ceramic primers on bond strength to glass-ceramics: a systematic review and meta-analysis of in vitro studies. J Prosthet Dent

2024;131:392-402.
14. Quirino Ramos R, Mercelis B, Hassan Ahmed M, Peumans M, Carpena Lopes G, Van Meerbeek B. Shelf-life effect of silane-containing universal adhesive on bonding effectiveness to glass-ceramic. Int J Adhes Adhes 2024;134:103806.
15. Kamitsu T, Shimomura-Kuroki J, Shinkai K. Effect of viscosity of experimental universal adhesive on bond strength to dentin prepared with Er:YAG laser. Sci Rep 2023;13:7900.
16. Thiranukoon P, Klaisiri A, Sriamporn T, Swasdison S, Thamrongananskul N. Does silane application affect bond strength between self-adhesive resin cements and feldspathic porcelain? J Compo Sci 2025;9:52.
17. Costa AJME, Burgoa S, Pinhata-Baptista OH, Gutierrez V, Cortes ARG. Digital workflow for image-guided immediate implant placement by using the socket-shield technique and custom abutment in the esthetic area. J Prosthet Dent 2023;130:155-9.
18. Guimarães HAB, Cardoso PC, Decurcio RA, Monteiro LJE, de Almeida LN, Martins WF, Magalhães APR. Simplified surface treatments for ceramic cementation: use of universal adhesive and self-etching ceramic primer. Int J Biomater 2018;2018:2598073.
19. Prado M, Prochnow C, Marchionatti AME, Baldissara P, Valandro LF, Wandscher VF. Ceramic surface treatment with a single-component primer: resin adhesion to glass ceramics. J Adhes Dent 2018;20:99-105.
20. Dimitriadi M, Zinelis S, Zafiropoulou M, Silikas N, Eliades G. Self-etch silane primer: reactivity and bonding with a lithium disilicate ceramic. Materials (Basel) 2020;13:641.
21. Cardenas AFM, Quintero-Calderon AS, Siqueira FSF, Campos VS, Wendlinger M, Pulido-Mora CA, Masson-Palacios MJ, Sarmiento-Delgado ML, Loguercio AD. Do different application modes improve the bonding performance of self-etching ceramic primer to lithium disilicate and feldspathic ceramics? J Adhes Dent 2019;21:319-27.
22. Rodrigues CDS, Grangeiro MTV, Assi RASDS, Santos MGD, Bottino MA, Melo RM. Self-etching primer or hydrofluoric acid: effects on the bond strength stability of a leucite-based glass-ceramic. J Adhes Dent 2025;27:115-22.
23. Moreira PM, Carvalho GLM, de Castro Albuquerque R, André CB. Effect of hydrofluoric acid and self-etch ceramic primers on the flexural strength and fatigue resistance of glass ceramics: a systematic review and meta-analysis of in vitro studies. Jpn Dent Sci Rev 2024;60:198-210.
24. Vichi A, Fabian Fonzar R, Carrabba M, Louca C, Scotti N, Mazzitelli C, Breschi L, Goracci C. Comparison between hydrofluoric acid and single-component primer as conditioners on resin cement adhesion to lithium silicate and lithium disilicate glass ceramics. Materials (Basel) 2021;14:6776.
25. Lopes GC, Perdigão J, Baptista D, Ballarin A. Does a self-etching ceramic primer improve bonding to lithium disilicate ceramics? Bond strengths and FESEM analyses. Oper Dent 2019;44:210-8.
26. Pang NS, Jung BY, Roh BD, Shin Y. Comparison of self-etching ceramic primer and conventional silanization to bond strength in cementation of fiber reinforced composite post. Materials (Basel) 2019;12:1585.
27. Vila-Nova TEL, Moura DMD, Araújo GM, Pinto RAS, Leite FPP, Melo RM, Özcan M, Souza ROAE. Effect of adhesive resin application on the durability of adhesion to CAD/CAM glass-ceramics after either hydrofluoric acid etching or self-etch primer application. J Adhes Dent 2022;24:279-89.
28. Liu J, Tu S, Wang M, Chen D, Chen C, Xie H. The influence of different factors on the bond strength of lithium disilicate-reinforced glass-ceramics to resin: a machine learning analysis. BMC Oral Health 2025;25:256.
29. Cinar S, Altan B, Akgungor G. Comparison of bond strength of monolithic CAD-CAM materials to resin cement using different surface treatment methods. J Adv Oral Res 2019;10:120-7.
30. Bahadır HS, Bayraktar Y. Evaluation of the repair capacities and color stabilities of a resin nanoceramic and hybrid CAD/CAM blocks. J Adv Prosthodont 2020;12:140-9.
31. Kömürcüoğlu MB, Sağırkaya E, Tulga A. Influence of different surface treatments on bond strength of novel CAD/CAM restorative materials to resin cement. J Adv Prosthodont 2017;9:439-46.
32. da Silva SEG, de Araújo GM, Souza KB, Moura DMD, Aurélio IL, May LG, Vila-Nova TEL, Zhang Y, de Assunção E Souza RO. Biaxial flexure strength and physicochemical characterization of a CAD/CAM lith-

https://doi.org/10.4047/jap.2026.18.2.131

ium disilicate ceramic: effect of etching time, silane, and adhesive applications. Clin Oral Investig 2022;26:6753-63.
33. Beyabanaki E, Eftekhar Ashtiani R, Feyzi M, Zandinejad A. Evaluation of microshear bond strength of four different CAD-CAM polymer-infiltrated ceramic materials after thermocycling. J Prosthodont 2022;31:623-8.
34. Park JH, Choi YS. Microtensile bond strength and micromorphologic analysis of surface-treated resin nanoceramics. J Adv Prosthodont 2016;8:275-84.
35. Yao C, Yang H, Yu J, Zhang L, Zhu Y, Huang C. High bond durability of universal adhesives on glass ceramics facilitated by silane pretreatment. Oper Dent 2018;43:602-12.
36. Yim KY, Beh YH, Goo CL. Effects of surface treatment and thermocycling on the shear bond strength of zirconia-reinforced lithium silicate ceramic. J Adhes Dent 2023;25:125-32.
37. Malysa A, Wezgowiec J, Grzebieluch W, Danel DP, Wieckiewicz M. Effect of thermocycling on the bond strength of self-adhesive resin cements used for luting CAD/CAM ceramics to human dentin. Int J Mol Sci 2022;23:745.
38. Calixto ET, Kelmer VF, Komegae GH, Pacheco RR, Pini N, Sundfeld D. Influence of varied silane commercial brands and adhesive application on bond strength and stability to lithium disilicate glass ceramic. Oper Dent 2024;49:325-35.
39. Arkoy S, Ulusoy M. Effect of different surface treatments on repair bond strength of CAD/CAM resin-matrix ceramics. Materials (Basel) 2022;15:6314.